Novel spin lattice in Cu_3TeO_6: an antiferromagnetic order and domain dynamics

2005 J. Phys.: Condens. Matter 17 7667

(http://iopscience.iop.org/0953-8984/17/48/017)

INSTITUTE OF PHYSICS PUBLISHING JOURNAL OF PHYSICS: CONDENSED MATTER

J. Phys.: Condens. Matter **17** (2005) 7667–7679 doi:10.1088/0953-8984/17/48/017

Novel spin lattice in Cu_3TeO_6: an antiferromagnetic order and domain dynamics

M Herak[1], H Berger[2], M Prester[1], M Miljak[1], I Živković[1], O Milat[1], D Drobac[1], S Popović[3] and O Zaharko[4]

[1] Institute of Physics, POB 304, HR-10 000, Zagreb, Croatia
[2] Institute de Physique de la Matière Complexe, EPFL, CH-1015 Lausanne, Switzerland
[3] Faculty of Science, Physics Department, Bijenička cesta 32, HR-10 000 Zagreb, Croatia
[4] Laboratory for Neutron Scattering, ETHZ and PSI, CH-5232 Villigen, Switzerland

Received 8 September 2005, in final form 14 October 2005
Published 11 November 2005
Online at stacks.iop.org/JPhysCM/17/7667

Abstract

We report on the magnetic properties of an insulating cubic compound Cu_3TeO_6 studied by ac and dc susceptibility, torque magnetometry and neutron powder diffraction. A novel three-dimensional magnetic lattice composed of almost planar regular hexagons of Cu^{2+} $S = 1/2$ spins is present in Cu_3TeO_6. The magnetic susceptibility in the paramagnetic state obeys the Curie–Weiss law in the 200–330 K regime with $\Theta_{CW} = -148$ K and at $T_N = 61$ K system undergoes an antiferromagnetic phase transition. Above T_N the susceptibility is isotropic. Below T_N a large anisotropy develops in fields $H \geqslant 500$ Oe. Torque measurements reveal the presence of antiferromagnetic domains below T_N. In a rather low magnetic field ($\gtrapprox$500 Oe) switching of domains is observed. The dynamics related to movement of domain walls is very slow at low temperatures (of the order of 10^2 s) and interferes with all torque measurements. The presence of domains is a consequence of the symmetry of the underlying magnetic lattice. Neutron powder diffraction reveals that antiferromagnetic long-range order is associated with the wavevector $\vec{k} = (0, 0, 0)$. The dominant component of the magnetic moment is along one of the $\langle \pm 1 \pm 1 \pm 1 \rangle$ space diagonals of the cubic unit cell, but it is not possible to resolve whether the structure is collinear or canted.

1. Introduction

Magnetism relying on $3d^9$ copper Cu^{2+} ions reveals a striking diversity of magnetic structures. This diversity originates from a broad range of effective magnetic dimensionalities characterizing various $3d^9$ magnetic systems [1]. Depending, in turn, on the level of frustration and the importance of quantum fluctuations, either singlet non-magnetic, disordered spin liquid or magnetically long-range ordered ground states set in at low temperatures. Understanding

the magnetic structures underlying each of these ground states represents an issue of central interest for $3d^9$-magnetism, as well for magnetism in general.

The existence of antiferromagnetic domains and domain dynamics in antiferromagnetically ordered materials is still a not well understood phenomenon. A large part of the work on that subject has been devoted to the behaviour of AFM/FM layers in connection to the exchange bias phenomenon, which is of great technological importance (see for example [2] and the references therein).

In this paper we present magnetic susceptibility, torque magnetometry and neutron powder diffraction studies of a copper tellurium oxide, Cu_3TeO_6. Apart from the crystal structure determination, published for the first time in 1968 [3] and revised in 1978 [4], no other properties of Cu_3TeO_6 have, to the best of our knowledge, ever been reported in literature. In this work we focus particularly on the magnetic ordering which sets in at 61 K. By scrutinizing the crystal structure and neutron diffraction data of Cu_3TeO_6, a novel type of 3D magnetic lattice has been identified. The symmetry of this lattice is such that it allows four antiferromagnetic domains with different orientation to coexist in the ordered state. The direction of spins is found from neutron powder diffraction measurements. Our results confirm the presence of antiferromagnetic domains in the ordered state. Due to the slow dynamics of domain walls at low temperatures we were able to qualitatively capture the influence of magnetic field and temperature on the domain dynamics with the (static) torque method.

2. Experimental details

Single crystals of Cu_3TeO_6 were obtained by the HBr chemical transport method in sealed quartz tubes with temperature gradients of 600–550 °C and 450–500 °C respectively. The resulting prisms were 2 mm long and 1–2 mm wide. The room-temperature x-ray powder diffraction patterns were collected on a Philips automatic diffractometer. They could be indexed in the cubic space group $Ia\bar{3}$ ($a = 9.537(1)$ Å), as reported previously [3, 4].

High-resolution ac susceptibility was measured in the temperature interval 4.2–200 K by a commercial CryoBIND system. The amplitude of the ac fields in the latter technique is usually small (of the order of 1 Oe, typically) representing an important advantage in studies of any kind of spontaneous magnetic ordering. The dc susceptibility was measured by the Faraday method in the temperature range 2–330 K in a field of 5 kG.

The highly sensitive torque measurements were performed on a home-made torque apparatus on the same sample that was used for the susceptibility measurement. Two orientations of the sample were chosen for torque measurements, with field rotation in the (001) and $(1\bar{1}0)$ planes. The magnetic field applied in torque measurements at low temperatures was $\leqslant$1.2 kOe.

Neutron powder diffraction patterns were collected in the temperature range 1.5–70 K on the DMC diffractometer at SINQ, Switzerland, with neutron wavelength 2.568 Å.

3. Crystal structure

The unit cell of Cu_3TeO_6 consists of 8 regular TeO_6 octahedra and 24 copper ions. Details of the structure can be found in [4]. We focus our attention on the copper Cu^{2+} ions which carry spin $S = 1/2$. Each copper ion is surrounded by six oxygen ions forming a very irregular octahedron. The Cu–O distances and O–Cu–O angles in one octahedron are given in table 1. All 24 CuO_6 octahedra are equivalent but there are 12 mutually different orientations of octahedra in the unit cell. Each copper ion has four nearest neighbours at the distance of

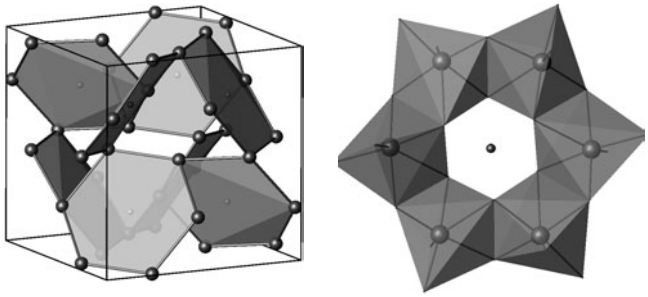

Figure 1. Left: magnetic lattice of the first copper spins 1/2 in Cu_3TeO_6. The larger spheres represent copper ions, and the smaller spheres tellurium ions. Oxygen ions are not drawn for the sake of clarity. Right: edge-sharing CuO_6 octahedra forming one hexagon in (a). The small sphere in the middle represents a tellurium ion.

Table 1. Cu–O distances and O–Cu–O angles characteristic for CuO_6 octahedra in Cu_3TeO_6.

Cu–O(i) (2x)	1.949(2) Å	Cu–O(ii) (2x)	2.031(2) Å	Cu–O(iii) (2x)	2.369(3) Å
O(i)–Cu–O′(i)	96.6(1)°	O(ii)–Cu–O′(ii)	95.5(2)°	O(iii)–Cu–O′(iii)	131.7(1)°
O(i)–Cu–O′(iii)	120.6(1)°	O(ii)–Cu–O(iii)	75.4(1)°	O(i)–Cu–O(ii)	85.6(1)°
O(ii)–Cu–O′(iii)	72.6(1)°	O(i)–Cu–O′(ii)	166.3(1)°	O(i)–Cu–O(iii)	91.9(1)°

3.18 Å (first nearest neighbours: 1st nns) and four more neighbours at 3.6 Å (2nd nn). When the 1st nn interaction is dominant, a new kind of spin lattice could be identified in Cu_3TeO_6, as shown in figure 1, right. In this spin lattice six copper ions form vertices of an almost planar hexagon centered around a tellurium ion with side length of 3.18 Å. Each hexagon plane is perpendicular to one space diagonal of the cubic unit cell, so there are four different orientations of hexagons. The lattice is formed in such a way that one hexagon (perpendicular to a certain space diagonal) is connected to six other hexagons (perpendicular to the other three space diagonals) by sharing vertices only. Each spin belongs to two hexagons and therefore has four 1st nns. The superexchange path to all 1st nns is established by edge sharing of CuO_6 octahedra with the Cu–O–Cu angles being 92.4° and 106.2°, as shown in figure 1, right.

Each spin also has four 2nd nns at a distance of 3.6 Å connected by sharing corners of CuO_6 octahedra with a Cu–O–Cu angle of 112.5°. If the 1st nn and 2nd nn superexchange interactions are similar in strength, the hexagon-based spin lattice would be better presented as in figure 2. This lattice can be compared to the pyrochlore lattice in which corner-sharing spin tetrahedra are present. The pyrochlore lattice is a 3D equivalent of the 2D Kagomé geometrically frustrated lattice. A consequence of strong geometrical frustration in those and similar systems is that there is no long-range order down to very low temperatures [5]. Geometrical frustration in those systems originates from the fact that spins in an equilateral triangular configuration with the antiferromagnetic coupling cannot simultaneously satisfy the interaction with all nearest neighbours. Since the sides of an irregular octahedron form six isosceles (3.18 Å–3.18 Å–3.6 Å) and two equilateral (3.6 Å–3.6 Å–3.6 Å) triangles (see figure 2, right) and all interactions are assumed to be antiferromagnetic, one would expect geometrical frustration to be present in such a lattice. In the pyrochlore lattice all triangles that form tetrahedra are equilateral. For the lattice in figure 2 some triangles are isosceles, and the superexchange between 1st and 2nd nns is certainly different, even if it is similar in strength. This should relieve frustration that would be strong if all triangles were equilateral and the superexchange was equal. Since here we are dealing with Heisenberg isotropic spins 1/2 and

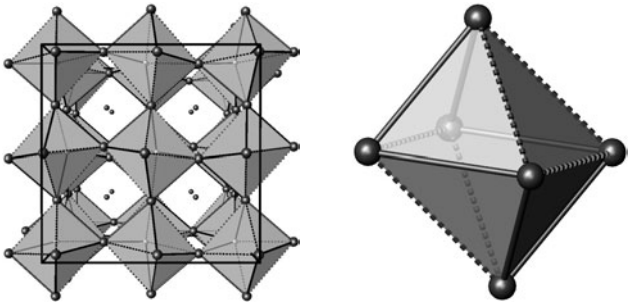

Figure 2. Left: magnetic lattice of copper ions when both 1st nn (at a distance 3.18 Å) and 2nd nn (at a distance 3.6 Å) interactions are considered. Solid lines represent 1st nns and dashed lines 2nd nns. The triangular arrangement of copper ions with AFM interaction should lead to geometrical frustration, if the superexchange between both 1st nns and 2nd nns were similar in strength. Right: one copper octahedron.

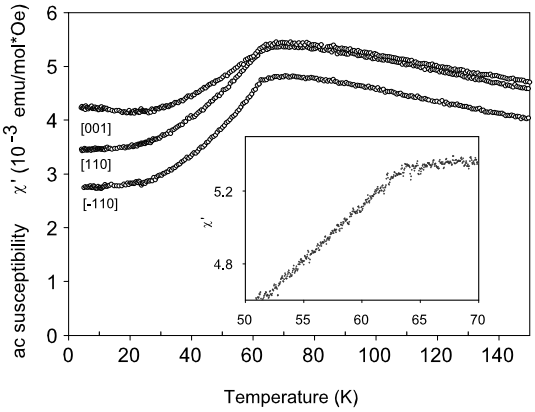

Figure 3. Main panel: ac susceptibility measurements on a single-crystalline Cu_3TeO_6 sample. Applied ac field (2 Oe, 430 Hz) was directed along the specified crystallographic directions. The vertical downward shift for the $[\bar{1}10]$ sample orientation is an artefact of the limited absolute accuracy of the ac susceptibility technique (see text). Inset: magnetic transition on an expanded scale.

not anisotropic Ising spins, there is a possibility of achieving some noncollinear long-range order at sufficiently low temperatures in a similar manner as Heisenberg spins on a triangular lattice arrange in an uniquely defined 120° ground state [5]. However, there is no experimental evidence for such a scenario in Cu_3TeO_6, as will be shown in section 4. This suggests that the 1st nn interaction is dominant and the spin lattice is the 3D lattice of Cu^{2+} corner-sharing hexagons [6].

4. Results

4.1. Magnetic measurements

The low-field ac susceptibility is shown in figure 3. A kink at about 61 K is a clear indication of 3d long-range magnetic ordering, presumably of an antiferromagnetic origin. A relative susceptibility change $((\chi_{70\,\mathrm{K}} - \chi_{5\,\mathrm{K}})/\chi_{70\,\mathrm{K}})$ of 0.21, 0.35 and 0.43 for the three crystal

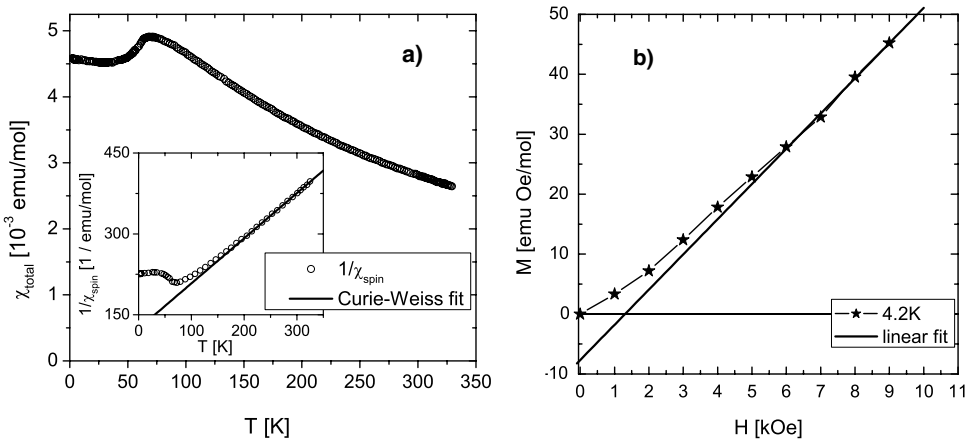

Figure 4. (a) Temperature dependence of dc susceptibility of Cu_3TeO_6 measured in $H = 5$ kOe. Inset: inverse spin susceptibility and Curie–Weiss law fit. (b) Magnetization versus H at 4.2 K. The linear curve is obtained by fitting M versus H from 6 to 9 kOe. Note the negative intercept and the deviation of low-field slope from this curve.

orientations indicated in figure 3 has been determined. Many other crystal orientations have been checked as well. All the results are characterized by a relative susceptibility change kept within the interval 0.2–0.4. Compared with classical antiferromagnets revealing Néel order, one notes the absence of pronounced susceptibility anisotropy: in a uniformly Néel-ordered system the relative susceptibility change reaches a value close to 1 for the field aligned along the sublattice magnetization axis while for the perpendicular field the susceptibility hardly changes [7] (relative change close to 0). Although the experimental results shown in figure 3 provide versatile information on *relative* susceptibility behaviour (i.e., its temperature dependence) they are limited by the poor *absolute* accuracy of the ac susceptibility (mutual inductance) technique. Thus the downward shift for the $[\bar{1}10]$ sample orientation, with respect to the results for other two orientations, can be attributed to experimental inaccuracy at the 10% level. This inaccuracy level seems quite realistic considering the very small sample signals involved in these measurements. The latter interpretation is consistent with small anisotropy (at a level much below 10%) found to characterize the paramagnetic state, as determined by our dc torque magnetometry studies presented below; as far as absolute accuracy is concerned, the ac susceptibility is known to be inferior to the dc one.

Figure 4(a) shows the total dc magnetic susceptibility in the broad temperature range. The spin susceptibility χ_{spin} was calculated by subtracting the temperature-independent part χ_0. χ_0 sums the diamagnetic susceptibility of all ions and the paramagnetic Van Vleck contribution of Cu^{2+}, thus $\chi_0 = +1.5 \times 10^{-4}$ emu mol^{-1}. At approximately 200 K a deviation from the Curie–Weiss law sets in. The inset to figure 4 shows that χ_{spin} follows the Curie–Weiss law, $1/\chi_{spin} = (T - \Theta_{CW})/C$, in the temperature range 200–330 K. The fit gives the values $C = 1.194 \pm 0.003$ emu K mol^{-1} for the Curie constant and $\Theta_{CW} \approx -148$ K for the Curie–Weiss temperature, respectively. Large and negative Θ_{CW} suggests that the Cu^{2+} spins $S = 1/2$ are strongly antiferromagnetically coupled. The value of g-factor calculated from the determined C is $g = 2.059 \pm 0.003$. This value is smaller than the value of $\langle g \rangle = 2.15$ characterizing a large number of investigated copper oxides. This implies that there is an approximately $\leqslant 5\%$ copper spin-deficiency in our sample. Below $\approx$200 K the susceptibility increases less rapidly than the high temperature Curie–Weiss law, reveals a maximum at 69 K and then decreases rapidly below 61 K, signifying a magnetic phase transition.

The magnetic phase transition at 61 K can be attributed to a long-range antiferromagnetic ordering, but not simple Néel order. Figure 4(b) shows the magnetization versus magnetic field H at 4.2 K. Clearly, the magnetization displays nonlinear behaviour in the investigated field region. In the low-field region $\leqslant$1 kOe, the magnetization is linear and extrapolates to zero for $H = 0$. In contrast, the high-field slope, which is $\approx$2 times larger, extrapolates to the negative intercept on the magnetization axis. Such anomalous magnetization behaviour is not consistent with a possible spin–flop transition. Rather, it is consistent with the presence of domains and their rotation caused by field H. In dc susceptibility measurements $\chi = M/H$, so the increase of slope of M versus H curve represents an increase of χ with field, which is characteristic behaviour of a system with domains. The domain picture is fully supported by the torque measurements.

In the paramagnetic ($T > 61$ K) regime, the torque reveals a very small anisotropy ($\approx 3 \times 10^{-6}$ emu mol^{-1}), as compared to 10^{-4} emu mol^{-1} in other copper oxides. This implies that the susceptibility is isotropic in Cu_3TeO_6 above T_N. In this insulating compound the main contribution to the susceptibility comes from copper spins. In the paramagnetic regime there are only two anisotropic contributions to the susceptibility: the temperature-dependent spin contribution via the g-factor anisotropy and the temperature-independent Van Vleck orbital contribution. Our method is sensitive enough to easily detect the usual g-factor anisotropy of copper spin. High isotropy suggested from the torque in Cu_3TeO_6 above T_N implies that either (i) the g-factor and the orbital contribution are isotropic or (ii) there is more than one set of Cu^{2+} magnetic axes in Cu_3TeO_6 but this anisotropy averages out in the net contribution. Taking into account the 12 different orientations of CuO_6 octahedra in the unit cell and the anisotropy of the g-factor in copper oxides, the case (ii) is probably realized in Cu_3TeO_6.

At low temperatures ($T < 61$ K) a large anisotropy develops in fields $H > 500$ Oe, as evidenced from the increase of the torque amplitude. In figures 5(a) and (b), torque curves are shown for two different orientations of the sample measured at 4.2 K. The field was rotated in the (001) (figure 5(a) and (110) 5(b)) planes, respectively. Due to the linear response of induced magnetization to the field in both paramagnetic and antiferromagnetic phase the measured torque Γ is given by

$$\Gamma = m/(2M_{\mathrm{mol}})(\chi_{\max} - \chi_{\min})H^2 \sin(2\phi + 2\phi_0) \tag{1}$$

for field H being in the plane perpendicular to the measured torque. m is the mass of the sample, M_{mol} is the molar mass, and $\chi_{\max}$ and $\chi_{\min}$ are maximal and minimal susceptibilities in the plane in which H is rotated. ϕ is the field goniometer angle and ϕ_0 is the phase difference between zero of the torque and zero of the field goniometer. The sample is mounted in such a way that the angle between the crystal axes and the field goniometer axes is known. As can be seen in figure 5, for none of the sample orientations does the torque follow the $\sin 2\theta$ curves entirely. Rather, a transition from one sine curve to another is observed. The two sine curves in both 5(a) and (b) have a phase difference of 90°, but in (b) the change of amplitude is larger. This behaviour reminds one of spin–flop in a single-domain antiferromagnet; however, the large hysteresis observed when rotating the magnetic field in the opposite direction suggests this is not the case. We performed measurements for several different orientations of the sample and obtained the same spin–flop like behaviour of all torque curves at $H \geqslant 500$ Oe. In some cases there was no change of phase, but only a reduction of amplitude. In fields $\leqslant$500 Oe this behaviour was not observed, but one more similar to the curve described in equation (1). In agreement with what is observed in magnetization and since spin–flop can be ruled out this behaviour of the torque can be attributed to the existence of several antiferromagnetic domains. By applying fields $\geqslant$500 Oe part of the domains has an energetically less favourable direction and can be switched to one more favourable in field but otherwise equivalent. This switching

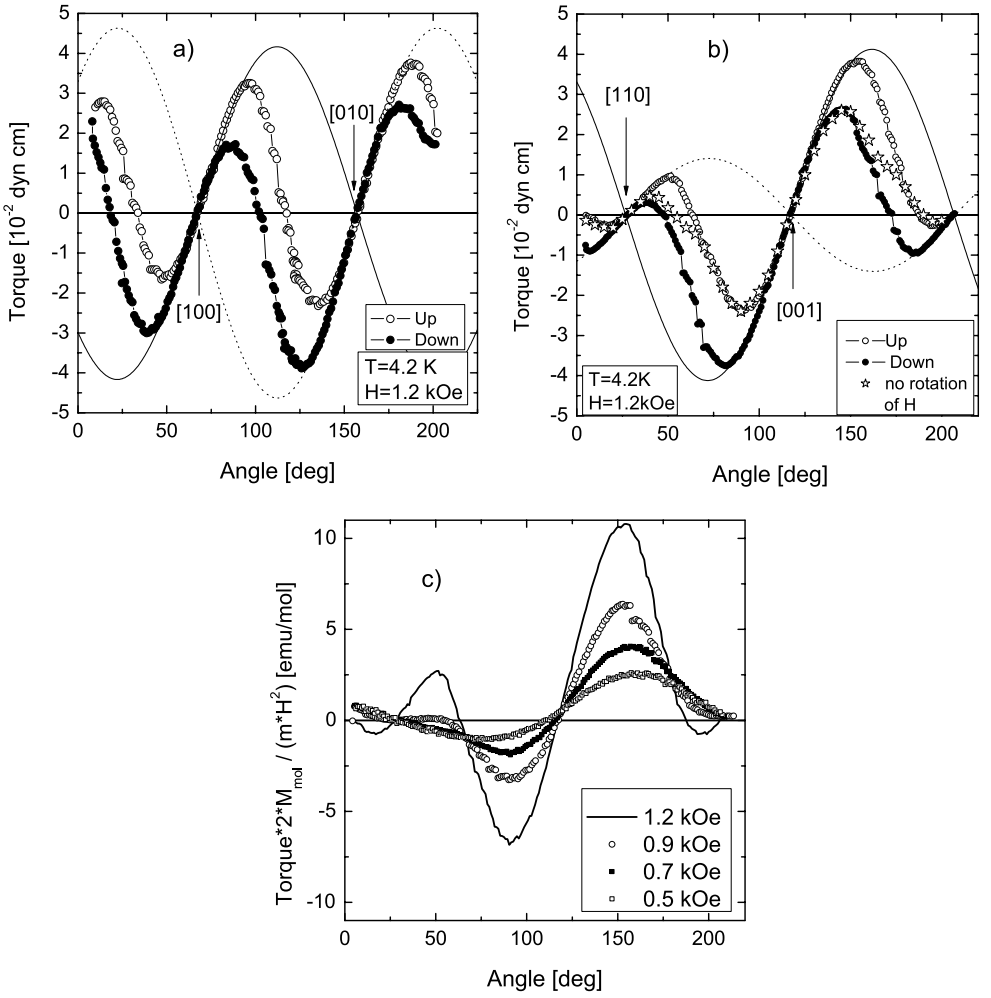

Figure 5. (a) Torque curve measured at 4.2 K with field $H = 1.2$ kOe rotating in the (001) plane. Empty circles represent measured data for rotating the field from 7° to 200° (up), and full circles back from 200° to 7° (down). Sine curves sketched by the solid and dotted lines represent torque curves that are usually obtained in an AFM single-domain state. (b) Torque curve measured at 4.2 K with field $H = 1.2$ kOe rotating in the (110) plane. The measured points labelled as stars are each obtained separately by sweeping the field from 0 to 1.2 kOe. (c) Torque curves measured at 4.2 K in fields 1.2, 0.9, 0.7 and 0.5 kOe for the same orientation as in (b). For the sake of clarity only one direction of the rotation of the field (up) is shown. For a single-domain Néel antiferromagnet $\Gamma \cdot 2 \cdot M_{\rm mol}/(m \cdot H^2)$ does not depend on the field strength for fields below the spin–flop field (see text).

of domains is accompanied by the creation, displacement and annihilation of domain walls. Figure 5(c) shows measured torque curves in several fields H at $T = 4.2$ K multiplied by the factor $2 \cdot M_{\rm mol}/(m \cdot H^2)$ for the orientation of the sample as in 5(b). According to equation (1), the result of the multiplication is $\Gamma \cdot 2 \cdot M_{\rm mol}/(m \cdot H^2) = (\chi_{\rm max} - \chi_{\rm min}) \cdot \sin(2\phi + 2\phi_0)$, which is field independent and can be used to estimate the susceptibility anisotropy. From figure 5(c) it is obvious that as the field increases above 500 Oe, the anisotropy increases. This is in agreement with what is observed in magnetization versus field measurements (figure 4) and what is

generally observed as an increase of susceptibility with magnetic field in systems containing domains. At fields $\lessapprox$500 Oe the estimated anisotropy practically does not depend on field and is of the order of 10^{-4} emu mol^{-1} at 4.2 K for all sample orientations we have measured. In comparison with susceptibility results some information about the number of different domains and low-field configuration can be obtained. The susceptibility at temperatures just above T_N is $\approx 4.9 \times 10^{-3}$ emu mol^{-1}. If there are only two domains at least for some sample orientations at 4.2 K we should measure the development of anisotropy of the order of 10^{-3} emu mol^{-1} in low fields. This implies that the number of domains is $\geqslant 3$ and that they are oriented in space in such a way as to produce minimum anisotropy in low fields, as for example three mutually perpendicular domains would. Also, small anisotropy suggests that in zero field the amount of different domains is practically equal.

The switching of domains, i.e. the dynamics of domain walls, in Cu_3TeO_6 is so slow that it interferes with our static torque measurements. The step-like features in the hysteretic angle range of curves in figure 5 appeared due to slow dynamics combined with nonuniform speed of rotation of the magnet. The hysteresis observed in figure 5 when rotating the field in the plane of measurement and back was at least partly due to the slow dynamics. The timescale of the domain dynamics was comparable to timescales in our experiments and thus interfered with all torque measurements, as will be shown in what follows.

Figure 6(a) presents the temperature dependence of the torque from 1.7 to 95 K. This particular measurement was performed in a field $H = 1.2$ kOe at a fixed angle of 95° for the sample orientation as shown in figure 5(a). Above $T_N = 61$ K up to room temperature the torque is practically zero, signifying the already mentioned susceptibility isotropy. The zero torque amplitude above T_N is also observed for other sample orientations, including the one in figure 5(b). To comment on the results below T_N a description of measurement procedure is necessary. First the sample was cooled from room temperature to 1.7 K in zero field. Then a field of 1.2 kOe was applied and kept constant during the heating run. The points were taken when the temperature increased for a certain ΔT. The amplitude of the torque turned out to be very sensitive to the heating rate at low temperatures. Generally, the torque decreases as temperature increases, signifying the destruction of the ordered state due to increasing temperature fluctuations. Two unusual features appear, however. The first is the increase of the torque from 1.7 K to $\approx$2 K. This is connected to the already mentioned sensitivity to heating rate which was slower in that interval than in the rest of the temperature range. The second unusual feature is that the torque amplitude at 4.2 K and 95° obtained in the temperature run is different from the one observed in the angular measurements shown in figure 5(a) for the same angle and temperature. This second feature could in principle be produced by the misalignment of the sample between those two types of measurement, but that was ruled out by checking the torque versus angle curve at 4.2 K both before and after the temperature run. The dependence on heating rate also observed in other temperature measurements suggests that the dynamics of domains in Cu_3TeO_6 is comparable to timescales of our experiment, at least at low temperatures. For this reason we measured the time dependence of the torque amplitude at different temperatures below T_N. Figure 6(b) presents the time dependence of the torque amplitude at 4.2 K. The inset shows the torque versus angle curve for the chosen sample orientation and the vertical line represents the angle at which time measurements were performed. The time dependence of applied field H is also shown on the same timescale for comparison. The initial change of torque is due to change of field from 0 to 1.2 kOe. When kept in constant field the torque takes a rather long time (of the order of 10^2 s) to saturate. However, the saturation value corresponds to neither of the values obtained in angular torque measurements shown in the inset of figure 6(b). This is very similar to the already mentioned noncorrespondence of torque amplitudes in the temperature run. Both of these measurements

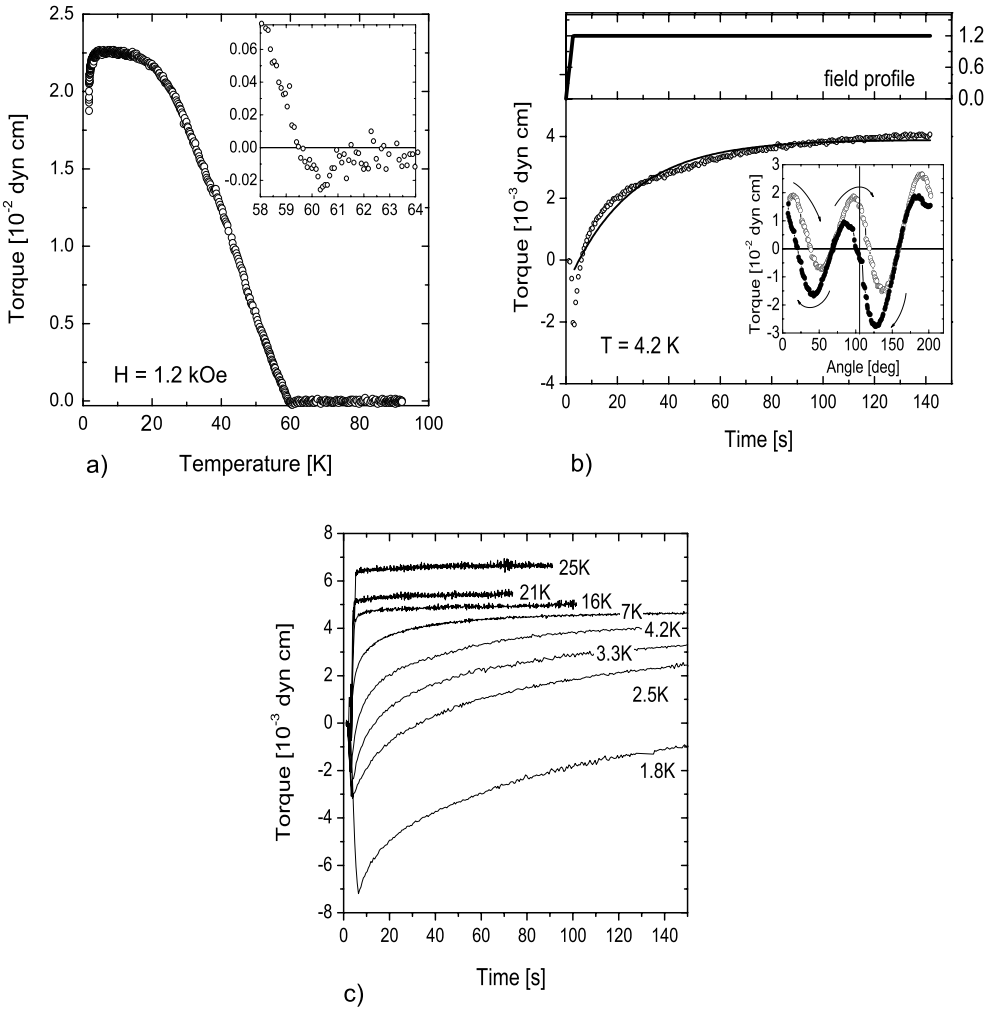

Figure 6. (a) Temperature dependence of the torque amplitude at 95° for the sample orientation as in 5(a) in a field of 1.2 kOe. The inset shows the narrow temperature range around the transition with the same axis labels. (b) Time dependence of the torque amplitude at 4.2 K in $H = 1.2$ kOe. The time dependence of the change of field is also shown (up). The full line represents the fit to $\Gamma = \Gamma_0 + (\Gamma_S - \Gamma_0)\,(1 - \exp(-(t - t_0)/\tau))$. The inset shows the angular dependence for chosen sample orientation and the vertical line represents the field angle at which the time measurements were performed. (c) Time dependence of the torque amplitude in $H = 1.2$ kOe for several temperatures below T_N and field orientation the same as in (b). The initial change of torque is due to the increase of the field from 0 to 1.2 kOe.

were performed in the angle range where large hysteresis was observed. We also checked the time dependence for angles in nonhysteretic parts of the curve, for example around the zero at 67°. In this case the time dependence was present but the net change of amplitude was smaller. Thus, nonhysteretic parts of the torque curves represent states where the net change of the anisotropy in the plane of measurement is small. The zero of the torque signifies that the configuration of the domains is such that the net anisotropy in the plane of measurement is zero.

In order to obtain the characteristic relaxation time at certain temperature we attempted to fit the torque versus time curves in constant field to the following form: $\Gamma = \Gamma_0 + (\Gamma_S - \Gamma_0)\ (1 - \exp(-(t - t0)/\tau))$, where t_0 is the moment the field reached constant value, Γ_0 is the initial value of the torque at $t = t_0$, Γ_S is the saturation value and τ is the characteristic relaxation time. The result of such a fit is shown in figure 6(b) by the solid line. The obtained τ is $\approx$25 s, but the proposed time dependence does not describe the time behaviour of the torque very well. The fit with two different relaxation times gave improved results, but it involved five free parameters which, under given circumstances, does not allow us to draw any conclusions from it. An attempt to quantitatively describe the dynamics failed, but the qualitative temperature behaviour of the relaxation time was captured, as shown in figure 6(c). Generally, as the temperature decreases the relaxation time increases. The time resolution of our torque method is $\gtrapprox$3 s, at best, which is why we do not observe any difference in time behaviour above 25 K. For temperatures below $\approx$4.2 K the torque does not saturate even after 150 s. Thus, there is a difference in measuring the torque amplitude after 10 s and after 100 s at low temperatures and that explains the sensitivity to heating rate. Slow heating rate means a longer time has passed between two subsequently measured points than would pass if the heating rate was faster. This is the reason why we observed a sharp increase at the beginning of many measurements whether they started at 1.7 or 4.2 K: the heating rate was slow enough to allow (the vicinity of) saturation to be reached.

The difference in torque amplitudes in angular measurements compared to those in temperature or time measurements obtained for identical experimental setup is also a consequence of the slow dynamics which makes the system sensitive to the history of measurement. This is clearly shown in figure 5(b). There are two ways to measure the angular dependence of the torque: by rotating the constant field while measuring (empty and full circles in figures 5(a) and (b)) or by measuring the torque versus field curve at a certain angle and then extracting the torque amplitude for a desired field value (empty stars in figure 5(b)). In the latter case the system always starts from the equilibrium configuration while in the former case that is true only for the first measured point. As can be seen, in the nonhysteretic part the torque is the same in both types of measurement. In the hysteretic part the former type of measurement can give larger amplitudes than the latter.

4.2. Neutron powder diffraction

Below $T_N = 61$ K magnetic peaks appear in neutron powder diffraction, figure 7(a), at the positions of the crystallographic reciprocal lattice corresponding to the wavevector $k = (0, 0, 0)$. The temperature variation of the integrated intensity of the magnetic peaks has classical behaviour; the intensities of the $\langle hkl \rangle$ and $\langle hk0 \rangle$ contributions vary as the square of the $S = 1/2$ Brillouin function.

The systematic extinction rules observed in the 1.5–70 K magnetic difference pattern (figure 7(a)) reveal that the I-translation is not combined with time reversal (hkl: $h+k+l = 2n$), while the glide planes are combined with it, if retained ($\langle hk0 \rangle$: $h, k = 2n$; $\langle hkl \rangle$ denotes cyclical permutation). Note that three-fold rotations are not compatible with time reversal. Our trials to find a model with cubic magnetic configuration symmetry were unsuccessful. Only models with trigonal symmetry gave good agreement to the observed diffraction pattern. The retention of the unique three-fold axis in the magnetic structure has two consequences. First, there must exist at least four orientation S-domains, each possessing its own $\langle 1 \pm 1 \pm 1 \rangle$ three-fold axis and each having a pair of 180° domains. Their presence is fully supported by the torque magnetometry results. Second, as the cubic symmetry is lost, the glide planes could not be elements of the magnetic group. The Cu^{2+} ions related by the glide planes must,

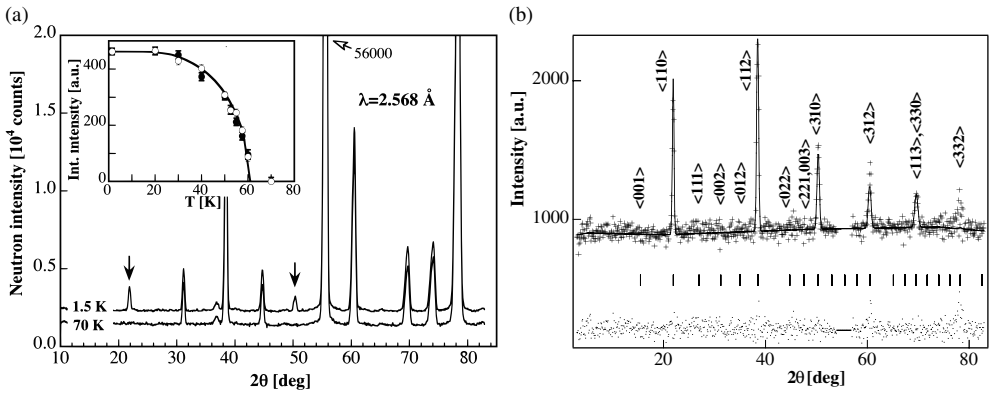

Figure 7. (a) DMC neutron powder diffraction patterns of Cu_3TeO_6. Arrows point to magnetic reflections. The inset shows the temperature evolution of the $\langle hk0\rangle$ (open circles) and $\langle hkl\rangle$ (filled circles) lowest angle magnetic peak intensity. (b) Observed 1.5–70 K magnetic difference pattern, calculated and difference patterns of Cu_3TeO_6 denoted by crosses, solid, and dotted lines, respectively. Note that the indices of the reflections are cyclically permutable.

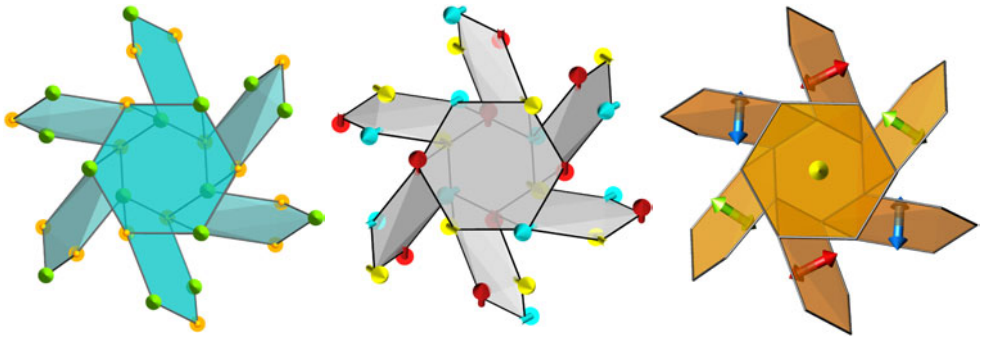

Figure 8. A fragment of the Cu magnetic moment arrangement as viewed along one of the space diagonals. Left: collinear antiferromagnetic model as one possibility for the magnetically ordered state in Cu_3TeO_6. In this model there are two sublattices with opposite direction of spins. Each spin from one sublattice has four 1st nns that belong to the other sublattice. Middle: noncollinear XXZ model as another possible candidate for long-range ordering in Cu_3TeO_6. There are six sublattices. The spins in the opposite corners of the hexagon belong to two collinear sublattices. The tilt of the spins is exaggerated to be more easily observable. Right: schematic view of antiferromagnetic domains realized in Cu_3TeO_6 due to symmetry.

(This figure is in colour only in the electronic version)

however, have their magnetic moments antiparallel to each other, otherwise magnetic intensity would be found at the hkl: $h + k + l = 2n$ positions.

The magnetic moment direction is not conditioned by extinctions and must be determined from modelling. Due to the high symmetry of the crystal lattice and the wavevector this task is, however, not easy, based on powder data alone [8]. For a collinear XXX antiferromagnetic model with spins aligned along the [111] direction and the 1.5 K moment value of 0.644(7) μ_B/Cu^{2+} a good fit ($R_M = 16.9\%$) has been obtained. The canted arrangements with magnetic moments tilted from the [111] direction fit the data equally well ($R_M = 13.2\%$). Figure 8 (left and middle) shows two of the possible models: XXX collinear antiferromagnetic state and XXZ canted arrangement. For the XXX model the spins

are aligned along one of the space diagonals of the cubic unit cell. Since each of the four orientations is equally possible, domains with four different spin orientations must coexist in the antiferromagnetically ordered state. In canted models the tilt of the spins from the [111] direction is small, of the order of 6°. Here also four equally probable antiferromagnetic orientation domains could exist. In this model the angle between two 1st nn moments is 168.7° (in the XXX model it is 180°) and between two 2nd nn moments it is 11.3° (in the XXX model it is 0°). Further neutron diffraction experiments on a single-domain crystal are needed to clarify these details.

5. Discussion

Magnetic susceptibility, torque and neutron diffraction measurements on an insulating cubic cuprate Cu_3TeO_6 have been reported for the first time. The magnetic lattice of this insulating compound is formed by copper spins 1/2. Each spin in the lattice has four 1st nns and four 2nd nns. If the superexchange interactions between 1st nns and 2nd nns are of similar strength and are antiferromagnetic, a rather strong geometric frustration should be present in this system. In geometrically frustrated systems long-range ordering appears only at temperatures $T_c \ll \Theta_{CW}$, where Θ_{CW} is the temperature obtained from the Curie–Weiss fit. The measure of frustration f is given by the phenomenological parameter $f = |\Theta_{CW}|/T_c$ [5]. Using quoted values for Θ_{CW} and T_N in Cu_3TeO_6, $f \approx 2$, suggesting that it is not strongly geometrically frustrated. This implies that the superexchange interaction between 1st nns is stronger than between 2nd nns and dominates the correlation between spins. Then the magnetic lattice can be viewed as a 3D lattice of strongly connected corner-sharing Cu^{2+} hexagons, i.e. rings of spins, in contrast to the Cu_3WO_6 structure, where loosely connected spin hexagons exist [9]. In Cu_3WO_6 the magnetic susceptibility implies a spin singlet ground state with a spin gap, unlike Cu_3TeO_6, which exhibits a 3D long-range AFM order. However, a rather early deviation of susceptibility from Curie–Weiss law at ≈170 K compared to $T_N = 61$ K is unusual for a 3D system. It is something that is usually observed in quasi-low-dimensional spin systems. Although the spin lattice in Cu_3TeO_6 extends in three dimensions, from figures 1 and 8 it is obvious that it is not a simple one. Each spin has four nearest neighbours in the spin lattice in figure 1. This is a rather low value for a 3D system and is in fact closer to values for low-dimensional systems. As is well known, the deviations from the Curie–Weiss law appear in practically all systems because of growing correlation length, i.e. the appearance of short-range order which is not accounted for in mean field theory. For low-dimensional systems with small coordination number the influence of short-range order is stronger, which is why the Curie–Weiss law in those systems is followed in a small temperature range, as compared to 3D systems with large coordination number ($\geqslant$6) where growing correlations start to have influence on susceptibility only at temperatures which are not far from T_N. This is why 3D systems in general obey the Curie–Weiss law in a larger temperature range than low-dimensional systems. Thus, the small coordination number of the spin lattice in figure 1 could be the reason for deviation from the Curie–Weiss law in Cu_3TeO_6: growing correlations have more influence on the susceptibility than they would if the coordination number was some usual 3D lattice value ($\geqslant$6). This can also be another reason for giving preference to the lattice in figure 1 instead of figure 2. The lattice in figure 2 has coordination number 8, which is sufficient for following the Curie–Weiss law behaviour to temperatures close to T_N.

All magnetic measurements suggest that the system does not behave as a single-domain antiferromagnet. Neutron measurements in zero field support this picture and reveal several possible models for long-range ordering, all comprising four orientation domains as an intrinsic property. The main component of the magnetic moment in one domain is along one of the space

diagonals of the cubic unit cell. A schematic presentation of all possible domains realized in Cu_3TeO_6 is shown in figure 8, right. There are four orientation domains and each of them has a pair of 180° domains, which makes $4 \times 2 = 8$ antiferromagnetic domains. The number of different kind of domain walls is $8 \times 7/2 = 28$.

In zero field and in low fields ($H \leqslant 500$ Oe) the number of different domains is approximately equal, as evidenced from the small torque amplitude, i.e. small anisotropy. Applying fields >500 Oe increases the measured torque (anisotropy), which suggests that the number of certain domains increases at the expense of others. This switching happens through movement of domain walls. At low temperatures the dynamics of domain walls slows down, as evidenced from the time dependence of the torque amplitude. At liquid helium temperatures the time needed for the torque to reach the saturation value in constant field is of the order of 10^1–10^2 s. Increasing the temperature helps depinning of domain walls which speeds up the dynamics. To get more quantitative results on the domain dynamics in Cu_3TeO_6 some method more suitable for measuring relaxation times should be employed.

References

[1] For a review, see *Quantum Magnetism* 2004 (*Springer Lecture Notes in Physics*) (Berlin: Springer) p 645
[2] Nogués J and Schuller I K 1999 *J. Magn. Magn. Mater.* **192** 203
[3] Hostachy A and Coing-Boyat J 1968 *C. R. Acad. Sci.* **267** 1435
[4] Falck L, Lindqvist O and Moret J 1978 *Acta Crystallogr.* B **34** 896
[5] Ramirez A P 2001 *Handbook on Magnetic Materials* vol 13, ed J H Buschow (Amsterdam: Elsevier Science) pp 426–520 and references therein
[6] More structural aspects of the magnetic lattice in Cu_3TeO_6 can be found on: http://mirta.ifs.hr/Cu3TeO6.html
[7] Any textbook on magnetism has a figure representing the susceptibility of antiferromagnetic ordered state, see e.g. Ashcroft N W and Mermin N D 1976 *Solid State Physics* (Philadelphia, PA: Saunders College) p 702
[8] Shirane G 1958 *Acta Crystallogr.* **12** 282
[9] Hase M and Uchinokura K 1995 *Physica* B **215** 325